Marks *et al. Metab Target Organ Damage* 2024;4:28
DOI: 10.20517/mtod.2024.44

Metabolism and Target Organ Damage

Review

Open Access

Noninvasive testing in the diagnosis of metabolic dysfunction-associated steatohepatitis

Lucas M. Marks[1], Thomas Jensen[2,#], Timothy R. DeGrado[3,#]

[1]Department of Radiology, VCU School of Medicine, Richmond, VA 23298-0470, USA.
[2]Department of Medicine, University of Colorado Anschutz Medical Campus, Aurora, CO 80045, USA.
[3]SpectronRx, Bunker Hill, IN 46914, USA.
[#]Co-senior authors.

Correspondence to: Dr. Thomas Jensen, Department of Medicine, University of Colorado Anschutz Medical Campus, 12801 E. 17th Ave. 7103 Research 1 South, Aurora, CO 80045, USA. E-mail: thomas.jensen@cuanschutz.edu

How to cite this article: Marks LM, Jensen T, DeGrado TR. Noninvasive testing in the diagnosis of metabolic dysfunction-associated steatohepatitis. *Metab Target Organ Damage* 2024;4:28. https://dx.doi.org/10.20517/mtod.2024.44

Received: 4 Jun 2024 **First Decision:** 5 Jul 2024 **Revised:** 29 Jul 2024 **Accepted:** 6 Aug 2024 **Published:** 22 Aug 2024

Academic Editor: Amedeo Lonardo **Copy Editor:** Dong-Li Li **Production Editor:** Dong-Li Li

Abstract

Metabolic dysfunction-associated steatotic liver disease (MASLD) [previously termed nonalcoholic fatty liver disease (NAFLD)] is estimated to be the most common chronic liver disease worldwide, affecting 25% of the world's population and becoming the leading cause of liver transplant in the US. The progression of MASLD from simple hepatic steatosis to the more severe metabolic dysfunction-associated steatohepatitis (MASH) [previously nonalcoholic steatohepatitis (NASH)] has critically important impacts on clinical outcomes. Early detection and staging of disease severity, along with lifestyle modifications and treatment of comorbid conditions, is the best way to prevent the progression or reverse the course of the disease. Although noninvasive imaging and predictive indices are available for the evaluation of hepatic fibrosis, the only way to diagnose MASH remains liver biopsy despite the risk for complications and being less desired by patients. Hence, there is a need to develop noninvasive tests to aid in both the diagnosis and monitoring of MASH, especially with the recent emergence of liver-directed therapy for "at risk" MASH (MASH with NAS ≥ 4 and Stage ≥ F2 Fibrosis). The goal of the current review is to cover the most recent pathophysiology, current diagnostic methods, and recent advances to aid in the diagnosis of MASH.

Keywords: Metabolic dysfunction-associated steatotic liver disease (MASLD), nonalcoholic fatty liver disease (NAFLD), metabolic dysfunction-associated steatohepatitis (MASH), imaging, fibrosis

INTRODUCTION

Metabolic dysfunction-associated steatotic liver disease (MASLD), previously nonalcoholic fatty liver disease (NAFLD), is the umbrella term for chronic liver disease that can range in severity from the simple hepatic steatosis of metabolic dysfunction-associated steatotic liver (MASL) to metabolic dysfunction-associated steatohepatitis (MASH), formerly nonalcoholic steatohepatitis (NASH), to overt cirrhosis, and eventually hepatocellular carcinoma (HCC)[1]. MASLD is now estimated to be the most common chronic liver disease globally, affecting 30% of the world's population[2] and is projected to soon become the leading indication for liver transplantation in the US[3]. There is active research into medications specifically used to treat MASLD/MASH[4]. Many of these medications, including Resmetirom, a thyroid hormone receptor analog that is the first FDA-approved medication in the management of MASLD, are primarily targeting the management of more progressive diseases including MASH and "at risk" MASH. Early detection and staging of disease severity, along with lifestyle modifications, treatment of comorbid conditions, and use of emerging novel agents, is the best way to prevent progression to more advanced disease. MASH has been associated with more rapid progression to end stage liver disease, the risk for hepatocellular carcinoma, diabetes, and cardiovascular disease compared with simple steatosis[5]. Hence, early detection can also offer motivation for providers and patients to earlier interventions with a better chance of success than later stages of fibrosis, which are more difficult to reverse. Unfortunately, the only method to confirm the diagnosis of MASH currently is through liver biopsy and histological examination. Despite intense interest, there remains a critical need for improved noninvasive biomarkers and imaging methods to help differentiate MASLD from MASH[2]. Imaging biomarkers in MASLD have been recently reviewed[6-8]. The goal of the current review is to briefly discuss diagnostic methods for MASLD/MASH, and recent advances in serum, predictive indices, and imaging that can differentiate MASH from simple liver steatosis.

EPIDEMIOLOGY AND CLINICAL SIGNIFICANCE OF MASLD

MASLD encompasses a spectrum of diseases, from mild simple hepatic steatosis to the more progressive form of MASH, which can progress to fibrosis, cirrhosis, and eventually hepatocellular carcinoma (HCC)[9-10]. Steatotic Liver Disease due to MASLD is diagnosed when there is ≥ 5% hepatic fat accumulation, accompanied by metabolic risk factors, and no other contributing causes[5]. In MASLD, there is both increased uptake of lipids into the liver from adipose tissue lipolysis and dietary sources, increased de novo lipogenesis, and compromised hepatic lipid transport[11,12]. Approximately 30%-40% of patients with MASLD will develop MASH, and subsequently, 40%-50% of patients with MASH will develop hepatic fibrosis, with a risk of progression to overt cirrhosis[13]. On average, patients with MASLD and MASH progress one histological stage of fibrosis every fourteen and seven years, respectively[14]. Hepatic fibrosis stage is the strongest predictor for disease-specific and overall mortality in patients with histologically confirmed MASH[15]. In addition, 25% of patients with MASH developed cirrhosis over a nine-year period[13]. In MASH, the risk of HCC is higher, with one study reporting incidence between 2.4% and 12.8% over a 3.2-year - 7.2-year period[16].

NONINVASIVE CLINICAL AND SERUM BIOMARKERS FOR MASH

Serum biomarkers

Basic biomarkers of MASH include a ratio between aspartate aminotransferases (AST) and alanine aminotransferase (ALT) of less than 1[2,17], ALT levels twice the upper limit of normal[18], and, with modest accuracy, plasma levels of cytokeratin 18 (CK18) fragments[19,20].

One investigational marker is the soluble macrophage activation marker CD136. This hemoglobin-haptoglobin scavenger receptor, expressed on monocytes and macrophages, was positively correlated with histologically confirmed MASH[21]. Another emerging biomarker is pro-collagen III (Pro-C3) levels that

indicate ECM turnover, an indirect measurement of active fibrogenesis[22]. One study indicated that this level was able to discriminate between hepatic steatosis and overt MASH, as well as the severity of MASH fibrogenesis[23]. Other individual markers that have shown promise in MASH detection include inflammatory markers such as TNF and IL-8, as well as hormones such as adiponectin and fibroblast growth factor 21 (FGF 21)[24]. Overall, these biomarkers are best at differentiating between mild fibrosis and advanced fibrosis/cirrhosis[2,17]. Despite the promising results of these serum markers, none has been proven to provide sufficient evidence for a conclusive diagnosis of MASH.

Predictive indices for MASLD and MASH

Several predictive indices using a multitude of components have been developed to predict the presence of MASLD/MASH. Although each index has shown some promise, none has been universally accepted as the standard for diagnosis[2,17]. The AST/Platelet Ratio Index (APRI), with limited evidence to date in MASLD, showed a sensitivity of 77% and a specificity of 72% in the identification of advanced fibrosis[2,17,25,26]. Two additional scores, the NAFLD fibrosis score (NFS) and Fib-4 score, have also been shown to accurately identify advanced fibrosis. For example, NFS has shown a positive predictive value (PPV) of 90% and a NPV of 93% for detecting advanced fibrosis. However, most markers, in general, appear to be limited in identifying MASH[17]. A study comparing seven different noninvasive markers and predictive indices for MASLD and fibrosis found the Fib-4 index to be the superior marker/index, but limited in diagnosing MASH[27]. A meta-analysis of common scores recently showed the APRI Score with an AUC of 0.83 (95%CI: 0.80, 0.86), a sensitivity of 0.45 (95%CI: 0.29, 0.62) with low certainty, and specificity of 0.89 (95%CI: 0.83, 0.92) with moderate certain for diagnosing MASH, and the BARD Score (BMI ≥ 28, AST, ALT, presence of Diabetes) an AUC of 0.74 (95%CI: 0.70, 0.77), a sensitivity of 0.72 (95%CI: 0.58,0.83), and specificity of 0.65 (95%CI: 0.55, 0.75) both with moderate certainty[28]. The NFS found an AUC of 0.82 (95%CI: 0.78, 0.85) in seven studies, a sensitivity of 0.30 (95%CI: 0.27, 0.33) in 795 patients with low certainty, and specificity of 0.96 (95%CI: 0.95, 0.96) in 2,749 patients with high certainty. Finally, the FIB-4 score found an AUC of 0.81 (95%CI: 0.77, 0.84), a sensitivity of 0.57 (95%CI: 0.39, 0.74), classified as low certainty because of reduced discriminatory performance and high inconsistency, and specificity of 0.89 (95%CI: 0.77, 0.95) with moderate certainty for identifying MASH.

Both the enhanced liver fibrosis panel (ELF) and the FibroSpect II panel are used to predict the extent of fibrosis in MASLD/MASH. The ELF panel included ECM turnover markers such as matrix metalloproteinase 1 (MMP-1), HA, and amino-terminal propeptide of type III collagen level and was found to have an accuracy of diagnosis for MASH with a cutoff value of 8.72, with a sensitivity of 0.714 and specificity of 0.741 (AUC = 0.74)[29]. FibroSure, a proprietary panel of six biochemical markers [Alpha-2-macroglobulin, Haptoglobin, Apolipoprotein A1, Gamma-glutamyl transpeptidase (GGT), Total bilirubin, and alanine aminotransferase (ALT)] showed low diagnostic value for MASH (AUROC = 0.59, se = 0.06; $P = 0.15$) and was not statistically significant[30]. NASH FibroSure, which includes FibroSure, ALT, triglycerides, and total cholesterol, had an AUC of 0.773 (95% confidence interval: 0.730-0.810), was confirmed in the control group 0.814 (0.774-0.847) and was superior to FIB-4, BARD, and NFS for diagnosing MASH[31]. In a retrospective study, FibroSpect II had a negative predictive value of 100% to rule out significant fibrosis in MASLD[32]. The OWLiver diagnostic predictor was established to be able to differentiate between normal liver and MASLD and between MASLD and MASH[33] and has been shown to have a diagnostic accuracy of 0.79[34]. OWLiver combines two panels of 25 different triglyceride markers with the patient's BMI and uses a liquid chromatography-mass spectrometry system to measure the relative intensities of the measured plasma triglycerides. Lastly, the MASHTest predictive index, the most comprehensive of the indices, uses age, sex, height, weight, serum triglycerides and cholesterol, macroglobulin, apolipoprotein A1, haptoglobin, gamma-glutamyl transferase, ALT, AST, and total bilirubin to identify MASH. Studies have found the index promising, with specificity, sensitivity, positive predictive

value, and negative predictive value of 94%, 33%, 66%, and 81%, respectively[35-37]. In addition, bone morphogenic 2 (BMP2), a glycoprotein found to belong to the transforming growth factor β (TGFβ) superfamily and found to be important in liver homeostasis, was found to be elevated in patients with MASH and an algorithm combined with age, gender, glucose, and GGT called the screening algorithm for NASH (SAN) was able to discriminate well from non-MASH patients (AUROC 0.886)[38]. Table 1 summarizes the diagnostic performance of the noninvasive tests for MASH.

Serum biomarker limitations

Despite the promising results of the serum biomarkers and predictive indices discussed above, no single noninvasive method has yet replaced liver biopsy for the confirmatory diagnosis and severe grading of MASH [Figure 1]. Several limitations persist with serum biomarkers or indices. For instance, normal aminotransferase levels may be observed in patients with advanced disease, and some indices are better suited for indicating the absence of advanced fibrosis rather than diagnosing MASH[12,39-41]. Additionally, some predictive indices are expensive commercial tests that are not widely available[24]. Another limiting factor of all noninvasive, non-imaging-based methods is that their cutoff values have not been validated in heterogeneous populations[42].

IMAGING BIOMARKERS OF MASH

Ultrasound-based imaging and magnetic resonance imaging

Vibration controlled transient elastography (VCTE) without or with controlled attenuation parameter (CAP) commonly reported in Fibroscan™ has generally performed poorly at diagnosing MASH. VTCE showed an AUC of 0.68 (0.62-0.74), and CAP had an AUC of 0.71 (0.65-0.76)[43]. In another cohort, two-dimensional (2D) shear-wave elastography (SWE), a risk score system using unweighted sum scores of attenuation coefficient and dispersion slope, showed an AUC of 0.94 (95%CI: 0.89, 0.98; $P < 0.05$) for diagnosing MASH, although it has not been further validated[44]. A recent review of magnetic resonance imaging (MRI) and magnetic resonance spectroscopy (MRS) has been shown to be an alternative to liver biopsy that can be used in longitudinal studies and as a guiding tool to assess treatment response in MASLD[45]. In particular, Abrigo *et al.* used ^{31}P MRS to assess mitochondrial metabolism by analyzing the ratio of inorganic phosphate to total phosphate ratio. They determined cutoffs that achieved a sensitivity and specificity of 91% and 91%, respectively, for diagnosing MASH[46]. MR elastography (MRE), which has been used to assess the degree of fibrosis, has not performed adequately in identifying MASH using 2D MRE, with an AUC of 0.75[47]. However, a proof-of-concept study has shown that multiparametric 3D MRE combined with MRI-PDFF holds promise as a longitudinal composite biomarker for MASH after weight-loss surgery[48]. A model based on coefficients derived from optical analysis of conventional non-contrast-enhanced MR images, known as NASHMRI, has demonstrated good diagnostic accuracy in MASLD patients, with an AUROC of 0.83 (95%CI: 0.75-0.92)[49]. This model could be particularly useful in centers lacking access to MRS or MRE. Additionally, a meta-analysis of iron-corrected imaging on MRI (cT1) has shown a good ability to discriminate the presence of MASH, with an AUROC of 0.78 (95%CI: 0.74-0.82)[50]. Table 1 summarizes these findings. Overall, US-based models appear limited in diagnosing MASH, while MR-based technologies, although promising, are expensive and have limited accessibility.

SPECT/PET mitochondrial dysfunction biomarkers: TSPO tracer

The translocator protein (18 kDa) (TSPO) (also known as peripheral-type benzodiazepine receptor, PBR) is a nucleus-encoded mitochondrial target transmembrane protein that binds cholesterol and various drugs and has been indicated in the modulation of mitochondrial function[51]. PET radiolabeled TSPO probes have enabled noninvasive and reliable investigations of neuropathological damages in experimental animals and humans[52]. Xie *et al.* investigated the TSPO PET probe [^{18}F]FEDAC in a methionine-choline-deficient (MCD) mouse model[53]. Hepatic uptake of [^{18}F]FEDAC increased with disease progression from simple

Table 1. Diagnostic performance of noninvasive techniques for evaluation of MASH

	Sensitivity	Specificity	PPV	NPV	AUROC
Predictive indices					
APRI[27]	0.45	0.89	0.63	0.79	0.83
NFS[27]	0.30	0.96	0.90	0.93	0.82
BARD Score[27]	0.72	0.65	0.64	0,73	0.74
Fib-4[27]	0.57	0.89	0.76	0.77	0.81
Enhanced liver fibrosis panel[28]	0.71	0.74	0.73	0.72	0.74
NASH FibroSure[29]	-	-	-	-	0.77-0.81
OWLiver[32,33]	0.73	0.80	0.79		0.81
NASHTest[34]	0.33	0.94	0.66	0.81	0.79
SAN[37]	0.54	0.96	0.86	0.83	0.886
Imaging biomarkers/techniques					
Ultrasound-based: VCTE[42]	0.61	0.59	0.83	0.31	0.71 with CAP
Ultrasound-based: 2D shear wave elastography[43]	-0.81	0.96	0.93	0.88	0.94
^{31}P MRS[45]	0.91	0.91	-0.95	-0.86	0.71
MRE[46]	NA	NA	NA	NA	0.73-0.75
MRINASH[48]	0.87	0.60	0.71	0.81	0.83
MRI cT1[49]	0.75	0.66	0.71	0.71	0.78
Imaging and biomarkers to identify "at risk" MASH					
FAST Score[82]	0.89	0.64	0.33-0.81	0.73-1.0	0.85
MAST Score[83] ≤ 0.165 ≥ 0.242	0.90 0.75	0.72 0.90	0.29 0.50	0.98 0.97	0.93
MEFIB[84] US Cohort Japanese Cohort	 NA NA	 NA NA	 0.97 0.91	 0.83 0.59	 0.90 0.84
FNI[85]	0.87-1.0	0.73-0.94	0.12-0.49	0.99-1.0	0.80-0.95
NIS2+™[86] ≤ 0.4564 ≥ 0.6815	 0.85 0.62	 0.61 0.85	0.77	0.83	0.81
MACK-3[87]	0.91	0.86	0.64	0.89	0.79

MASH: Metabolic dysfunction-associated steatohepatitis; PPV: positive predictive value; NPV: negative predictive value; AUROC: area under the receiver-operator curve; APRI: AST/Platelet Ratio Index; NFS: nonalcoholic fatty liver disease fibrosis score; Fib-4: fibrosis-4 index; NASH: nonalcoholic steatohepatitis; SAN: screening algorithm for NASH; VCTE: vibration controlled transient elastography; CAP: controlled attenuation parameter; MRS: magnetic resonance spectroscopy; MRE: Magnetic resonance elastography; MRI: magnetic resonance imaging; FNI: Fibrotic NASH Index; NA: not applicable.

steatosis to MASH ($P < 0.01$). A close correlation was identified between [^{18}F]FEDAC uptake ratio and necroinflammation in the liver (Pearson's $r = 0.922$, $P = 0.000$). Specific binding of [^{18}F]FEDAC to TSPO in the MASLD livers was shown in competition studies with the unlabeled TSPO-selective ligand PK11195. Autoradiography and histopathology confirmed the PET imaging results. Furthermore, the liver:blood ratios determined from biodistribution data correlated with TSPO and CD11b (macrophage and activated lymphocyte marker) mRNA levels as the steatohepatitis condition progressed over the 8-week period. Li *et al.* recently examined TSPO expression at all stages of MASLD in both human patients and mouse models of MASH[54]. TSPO immunoreactivity was low in normal livers but elevated in MASLD, MASH, and cirrhotic livers. After the removal of areas of blood and vessels, TSPO signal intensity was significantly higher in patients with steatosis, MASH, and cirrhosis than in controls, and this increase was proportional to the extent of liver pathology. In mouse models, the TSPO positive signal was highest in MASH samples. qPCR analysis indicated corresponding increases in TSPO mRNA expression, which gradually increased from control (1×) to steatosis (1.99×) to MASH (2.68×). Taken together, TSPO expression levels correlate

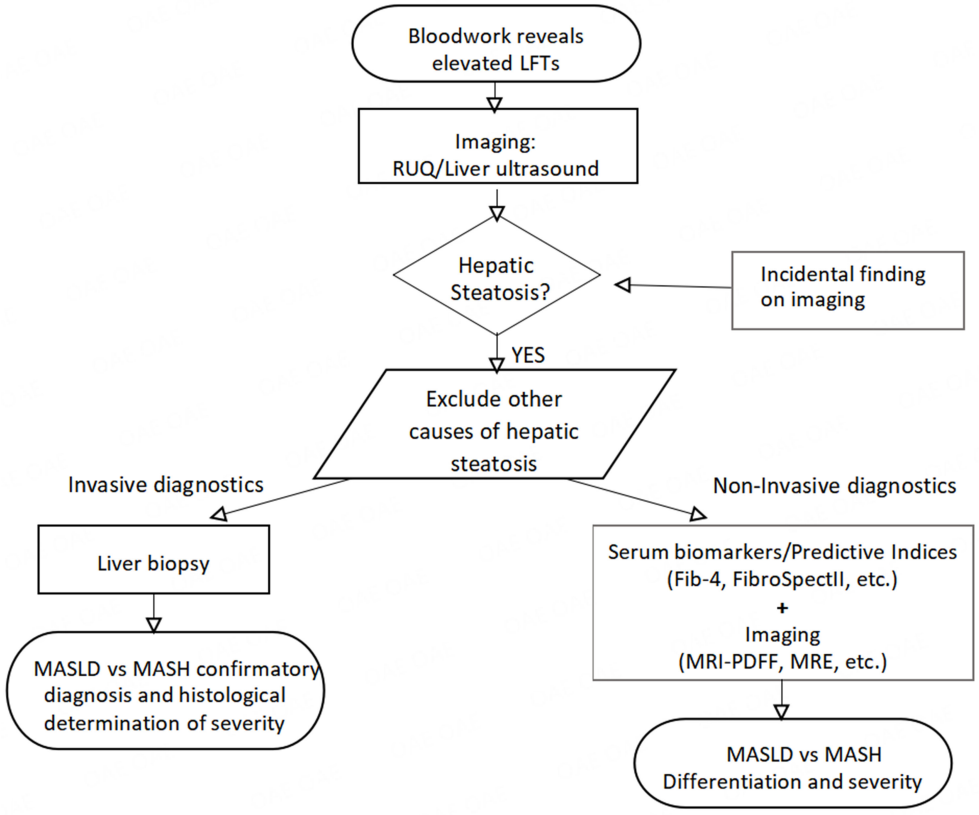

Figure 1. Example of a diagnostic workflow algorithm of MASLD/MASH. MASLD: Metabolic dysfunction-associated steatotic liver disease; MASH: metabolic dysfunction-associated steatohepatitis.

well with the degree of liver disease. Future studies in human MASLD and MASH are strongly encouraged as TSPO appears to be a promising imaging biomarker for the diagnosis and staging of MASLD.

SPECT/PET mitochondrial dysfunction biomarkers: mitochondrial membrane potential tracers

As previously noted, the respiratory chain of the inner mitochondrial membrane within hepatocytes undergoes dysfunction in the progression of MASLD in response to dysregulation of fatty acid oxidation and the increasing formation of ROS within the mitochondrial matrix. One of the indirect effects of mitochondrial damage is a decrease in the mitochondrial transmembrane potential[55]. The lipophilic cationic SPECT radiopharmaceutical Technetium-99 m-2-methoxy-isobutyl-isonitrile ([^{99m}Tc]MIBI), originally developed as a myocardial perfusion imaging probe, is a candidate imaging probe to noninvasively assess the mitochondrial membrane potential in MASLD[56,57]. Rokugawa *et al.* investigated the hepatic uptake of [^{99m}Tc]MIBI in the MCD MASH mouse model[56]. [^{99m}Tc]MIBI SPECT imaging clearly showed a decrease in hepatic [^{99m}Tc]MIBI retention in MCD-fed mice compared to control mice[56]. Clearance half-time after [^{99m}Tc]MIBI injection was significantly decreased in the liver of MCD-fed mice (control, MCD 2 weeks, and MCD 4 weeks, $T_{1/2}$ = 57.6, 37.6, and 19.8 min, respectively), although no change in time at peak activity was observed in MCD-fed mice. SPECT data and histological score showed a negative correlation (r = -0.74, $P < 0.05$) between $T_{1/2}$ and NAFLD activity score. These results support further investigations in human MASLD and MASH with [^{99m}Tc]MIBI SPECT imaging to detect hepatic mitochondrial dysfunction induced by steatosis and inflammation.

SPECT/PET mitochondrial dysfunction biomarkers: fatty acid metabolic tracers

As discussed previously, alterations of NEFA metabolism are observed in MASLD in both obese and non-obese patients with the development of lipotoxic metabolic intermediates. Various fatty acid imaging probes have been extensively studied in the context of myocardial imaging[56,58]. Fukumoto *et al.* investigated the use of the β-methylated pentadecanoic acid analog [^{123}I]BMIPP for SPECT imaging of MASH by virtue of its metabolism to complex lipids and clearance rate related to turnover of the labeled lipid pools[59,60]. A slower clearance rate (< 0.4%/min) of [^{123}I]BMIPP from the liver was observed in obese and non-obese MASH patients who also showed severe hepatic steatosis (> 50% fat fraction), while the clearance rate from less severe steatotic MASH liver was higher (> 0.4%/min). A higher clearance rate was restored by treatment with the peroxisome proliferator-activated receptor-α (PPAR-α) activator bezafibrate. They proposed that the hepatic clearance rate derived from SPECT imaging data after [^{123}I]BMIPP administration may serve as an indirect indicator of β-oxidation rate. Iozzo *et al.* employed the 6-thia substituted PET fatty acid probe, 17-[^{18}F]fluoro-6-thia-heptadecanoic acid ([^{18}F]FTHA), to perform PET imaging studies in patients with impaired glucose tolerance (IGT) or type 2 diabetes (T2D)[61], postulating that radiotracer uptake would serve as an indicator of exogenous NEFA uptake and metabolism in liver. Although the elevated glucose and insulin levels in IGT patients are known to impair splanchnic β-oxidation, the PET-derived measurement of FTHA accumulation could reflect changes in exogenous NEFA uptake and metabolism since FTHA is a metabolically trapped tracer. Quantitative estimates of the liver fractional NEFA extraction were found to be significantly reduced in IGT patients in comparison to controls and the same quantitative index was further decreased in type 2 diabetics. Although the metabolic fate of FTHA in liver had not been characterized, the authors suggest that decreased uptake in IGT and T2D is consistent with the downregulation of fatty acid oxidation through substrate competition and enhanced lipid synthesis and export from the liver. Liver pathology was not assessed in this study, so the relationship of the imaging findings to MASH was not evaluated. Iozzo *et al.* later studied PET imaging of [^{11}C]palmitic acid kinetics in liver in healthy and obese subjects[62]. [^{11}C]Palmitic acid is a direct analog of natural palmitate, so its kinetics can be interpreted as reflecting the uptake and metabolism of palmitate from the circulation. A 3-tissue compartment model was used to fit the time course of radioactivity concentration in liver tissue, using metabolite-corrected arterial and venous blood concentrations as dual inputs to the model. The fitted parameter estimates indicated that oxidation and esterification rates accounted for 40% and 60% of liver NEFA uptake, respectively. Uptake and esterification rates of exogenous palmitate were similar between healthy and obese subjects, but the estimated FA oxidation rate was increased about 2-fold in the liver of obese subjects (P = 0.0007). Hepatic NEFA oxidation was associated with circulating insulin levels, homeostatic model assessment index (HOMA), and adipose tissue insulin resistance. Visceral lipolysis rates determined from [^{11}C]palmitate arterial and portal venous plasma levels trended higher in obese subjects (P = 0.09). Liver pathology or blood markers of inflammation were not assessed. To our knowledge, this methodology has yet to be applied in the setting of MASH.

SPECT/PET inflammation biomarkers: [^{18}F]FDG-PET for glucose uptake/phosphorylation

The FDA-approved glucose analog PET probe, 2[^{18}F]fluoro-2-deoxy-D-glucose ([^{18}F]FDG), has been utilized in many contexts to detect and localize sites of tissue inflammation based on elevated glycolysis levels in infiltrating immune cells. The well-characterized metabolic handling and widespread commercial availability (at low cost) of [^{18}F]FDG make this an attractive option. Early work to apply [^{18}F]FDG-PET to imaging of hepatic inflammation in MASLD produced conflicting results[63-66] because of two main issues: (1) physiologic uptake and metabolism of [^{18}F]FDG in hepatocytes complicates the overall kinetics of radioactivity in liver tissue; and (2) since FDG does not accumulate in liver fat, the FDG uptake as measured by standardized uptake value (SUV) is dependent on liver fat fraction. Keramida *et al.* proposed to adjust the liver SUV for liver fat content by measuring liver CT density Hounsfield units (HUS) via PET/CT imaging[67]. An inversely linear relationship was found between CT density and fat percentage, which was

then used to correct the liver SUV. Without fat adjustment, liver SUVs were similar between subjects with and without steatosis. However, after fat adjustment, liver SUVs were significantly higher in subjects with steatosis, with a consistently higher SUV of ~0.4 g/mL across a wide range of fasting blood glucose levels[68]. To account for the potential effects of differences in blood [^{18}F]FDG concentrations at the time of measurement, ratios of SUVs in liver relative to blood (measured noninvasively in the left ventricle) also indicated higher accumulation of [^{18}F]FDG in MALSD. Liver pathology was not obtained to understand how the derived [^{18}F]FDG uptake indices relate to the severity of MASH. Sarkar *et al.* have recently developed a kinetic modeling technique that simultaneously optimizes parameters for modeling of the dual-blood supply of liver and [^{18}F]FDG kinetics in liver tissue[69,70]. The results were correlated to liver histopathology measurements for degree of inflammation according to the NASH Clinical Research Network criteria. Statistically significant decreases were found in the K1 uptake parameter for medium *vs.* low levels of inflammation and high *vs.* medium levels of inflammation[69]. The authors interpreted the negative correlation of K1 inflammation score to reflect decreased glucose transport with increased liver inflammation and injury in MASH secondary to inherent apoptotic processes[70]. However, their model did not adjust for fat fraction in the liver tissue. Therefore, the decreased rates of [^{18}F]FDG transport reflected in K1 values in MASH liver may have been influenced by increased steatosis. Future work will benefit from the standardization of methods for data acquisition and analysis of [^{18}F]FDG kinetics in liver.

SPECT/PET inflammation biomarkers: Kupffer cell phagocytosis tracers

Since hepatocytes and Kupffer cells (KCs) are affected by various liver disorders to a similar extent, colloid scintigraphy has long been used in the diagnosis and evaluation of numerous diseases causing diffuse liver involvement. Duman *et al.* investigated the use of scintigraphy and SPECT imaging with ^{99m}Tc tin colloid in patients with biopsy-proven MASH in the absence of cirrhosis[71]. Upon scintigraphy and SPECT, the liver right/left lobe ratio was altered in all patients, favoring the left over the right lobe. The authors proposed that the imaging findings were consistent with faster regeneration rates of the left lobe after toxic injury to the liver[72]. Slower blood clearance and lower ratios of liver/spleen and liver/bone marrow were also found in MASH subjects, consistent with slower KC sequestration of the colloidal radiotracer in MASH liver, allowing more radiotracer to be taken up in spleen and bone marrow macrophages. However, the lack of data in a group of patients with simple steatosis prevented the evaluation of this methodology to differentiate MASLD from MASH.

[^{99m}Tc]phytate was first introduced by Subramanian to evaluate reticuloendothelial activity in the liver and bone marrow[73]. It was found that the molecule acts as a nanoparticle, reacting with calcium in the serum and undergoing phagocytosis by reticuloendothelial cells of the mononuclear phagocyte system, especially by monocytes cells, macrophages, and Kupffer cells[62]. Based on the previous use of ^{99m}Tc-phytate scintigraphy for diagnosis and evaluation of liver diseases such as alcoholic steatohepatitis, Kikuchi *et al.* evaluated this radiotracer in 29 patients with biopsy-proven, early-stage MASH and 8 patients with simple steatosis (MASLD) that were matched for age, sex, and BMI[74]. Although serum ferritin levels were significantly higher in the MASH group, other routine biochemistry laboratory values were not significantly different between the MASLD and MASH groups. The liver/spleen ratio measured by ^{99m}Tc-phytate scintigraphy was used as an index of KC phagocytic dysfunction, showing a 37% reduction in the MASH group relative to the MASLD group. Conversely, the spleen/heart ratio was significantly increased in the MASH group, indicating activation of splenic macrophages in response to KC signaling[71]. A comparison study with the two colloidal radiotracers [^{99m}Tc]sulfur colloid and ^{99m}Tcphytate in patients having a spectrum of normal to advanced liver disease showed essentially similar uptake behavior of the two radiotracers in liver and bone marrow[75]. The former is used routinely in general nuclear medicine to evaluate various conditions, but its use for differentiation of MASLD from MASH has not been studied. Recently, ^{68}Ga-nanocolloid was introduced as a PET radiopharmaceutical for sentinel lymph node

imaging[76] and may have potential utility for the evaluation of KC phagocytic activity in the setting of MASH.

SPECT/PET inflammation biomarkers: thymidine phosphorylase tracers

Thymidine phosphorylase (TYMP) converts the nucleosides thymidine and deoxyuridine into thymine and uracil, respectively, within the nucleus of the cell. TYMP is induced by tumor necrosis factor-α (TNFα) in response to tissue inflammation and is typically overexpressed in several diseased conditions, including obesity, type 2 diabetes, and MASLD[77,78]. However, whether TYMP plays a role in the development of these diseases is unknown. Yue *et al.* recently published preliminary results that TYMP-deficient (TYMP-/-) male mice exhibited significantly limited body weight gain, as well as liver and perigonadal fat weights, when fed either a western diet or a pro-diabetic high-fat diet compared with wild-type mice[78]. TYMP deficiency also reduced the expression of enzymes that confer glycolysis and de novo lipogenesis in the liver and enhanced the sensitivity of primary hepatocytes to insulin as evidenced by the increase in AKT activation. Inhibition of TYMP with tipiracil, a selective potent TYMP inhibitor, dramatically reduced Western diet and high-fat diet-induced body weight gain. Higashikawa *et al.* developed a ^{123}I-labeled imaging probe for TYMP, [^{123}I]5-iodo-6-[(2-iminoimidazolidinyl)methyl]uracil ([^{123}I]IIMU), for diagnosis of MASH[79]. The hepatic expression levels of TYMP were found to be significantly lower in MCD MASH mouse model at both mRNA and protein levels, suggesting that a decrease in TYMP level could be an indicator of MASH. [^{125}I]IIMU was uniformly distributed in the liver of control mice, whereas it showed a patchy pattern in that of MASH mice. The hepatic uptake of [^{125}I]IIMU was concordant with the expression levels of TYMP protein in the liver of control and MASH mice. SPECT imaging studies with [^{123}I]IIMU showed 44% lower hepatic uptake in the MASH mice relative to controls. These results are positive for imaging evaluation of MASH and require follow-up studies to determine their effectiveness for noninvasive differentiation of MASLD and MASH.

IDENTIFYING "AT RISK" MASH

As mentioned earlier, identifying "at risk" MASH has gained increasing interest, particularly following the recent approval of Resmetirom. This approval was based on a Phase 3 Trial that demonstrated significant improvement in MASH resolution (without worsening of fibrosis) and/or an improvement in fibrosis by one stage or more[80]. As mentioned previously, liver biopsy has been considered the Gold Standard for diagnosing degree of MASLD. However, it has several limitations, including cost and risk of complications, high rates of intra- and inter-variability reads, as well as sampling variability due to the heterogeneous nature of MASLD and biopsies only representing 1/50,000 of the entire liver[81,82]. The development of noninvasive tests (NITs), typically involving a combination of serum biomarkers and/or imaging to identify "at risk" MASH, appears to be a useful tool for both clinical trial enrollment and patient treatment selection. The FAST Score, which is a combination of the CAP and LSM from Fibroscan™ and AST, has demonstrated a strong ability to distinguish "at risk" MASH. It has an AUROC of 0.85 (95%CI: 0.83-0.87) in a pooled validation cohort, with a threshold of ≤ 0.35 to rule out and ≥ 0.67 to rule in "at risk" MASH[83]. A similar score, combining PDFF, MRE Stiffness, and AST, known as the MAST Score, has also been shown to distinguish "at risk" MASH. It has an AUROC of 0.93 (95%CI: 0.88-0.97), with a cutoff of ≤ 0.165 for ruling out and ≥ 0.242 for ruling in ref[84]. Another tool relying on MRE is the MEFIB score, which combines an MRE LSM of ≥ 3.3 kPa and a FIB-4 of ≥ 1.6. This tool has been shown to effectively identify "at risk" MASH in both a United States (US) cohort and a Japanese cohort, with an AUROC of 0.90 (95%CI: 0.85-0.95) and 0.84 (95%CI: 0.78-0.89), respectively[85]. A recent study involving similar US and Japanese cohorts found that MEFIB is superior to both MAST and FAST in detecting "at risk" MASH with NAFLD activity score ≥ 4 and fibrosis stage ≥ 2. Specifically, MEFIB outperformed both MAST and FAST (both $P < 0.05$), with AUROC values for MEFIB, MAST, and FAST being 0.768 (95%CI 0.728-0.808), 0.719 (95%CI 0.671-0.766), and 0.687 (95%CI 0.640-0.733), respectively. A promising inexpensive screening tool, known

as the Fibrotic NASH Index (FNI), was developed based on AST, HDL, and A1c. This tool has demonstrated excellent ability to rule out "at risk" MASH, with a NPV ranging from 0.99-1.0 and AUROCs ranging from 0.80 (95%CI: 0.75-0.83) to 0.95 (95%CI: 0.92-0.98) in the validation cohort, though PPV only ranged from 0.12-0.49[86]. NIS2+™, which combines sex and the biomarkers miR-34a-5p and YKL-40, as well as sex *miR-34a-5p, has recently shown a reasonable ability to detect "at risk" MASH. It achieved an AUROC of 0.81 (95%CI: 0.80-0.83) with a NPV of 0.83 and a PPV of 0.77, using cutoffs of ≤ 0.4564 and ≥ 0.6815, respectively[87]. Finally, MACK-3, a score derived from three biomarkers (AST, homeostasis model assessment, and cytokeratin 18), has also demonstrated a reasonable ability to detect "at risk" MASH with an AUROC of 0.79 (95%CI: 0.77-0.81)[88]. Although many of these tools are not readily available to most clinicians, their capability to detect "at risk" MASH is likely to lead to increased usage, particularly among specialists managing patients with more advanced chronic MASLD.

CONCLUSION

Although liver biopsy is currently considered the gold standard for diagnosing MASH, including "at risk" MASH, recent advancements in imaging techniques with radiotracers related to metabolism, as well as new diagnostic scoring tools developed through clinical trials, show promise in potentially replacing liver biopsy for diagnosing and managing more advanced stages of MASLD. The use of NITs for identifying MASLD, particularly "at risk" MASLD, could be valuable for both clinical trial enrollment and patient selection for treatment. As reviewed, various biochemical features of MASLD and MASH underpin the different strategies used in noninvasive imaging techniques. Among these, imaging markers that target specific receptors or transporters, which are up- or downregulated in MASH compared to simple steatotic liver, show the most promise for further investigation. Particularly noteworthy are TSPO binders, mitochondrial membrane function, and thymidine phosphorylase, which appear to be especially promising for evaluating MASH. Clinical trials are underway to develop and validate a combination of imaging modalities, such as Fibroscan™ and MRE, along with serum biomarkers and anthropomorphic features associated with MASLD. These efforts aim to enhance clinical trial recruitment and provide NITs for clinicians to select patients for pharmacological agents advancing through the MASH pipeline, including the first approved medication, Resmetirom. The noninvasive imaging methods presented in this review offer hope that one or more of these methods could potentially replace liver biopsy in the diagnosis of MASH soon. Additionally, these imaging tools may be employed serially in patients, eliminating the need for repeated invasive biopsies to monitor disease progression and the effects of medical, lifestyle, or surgical interventions aimed at preventing progression to cirrhosis and HCC.

DECLARATIONS

Acknowledgments

The authors are thankful for support from the Department of Radiology, University of Colorado Anschutz Medical Campus.

Authors' contributions

Primary author of the review and initial framework: Marks LM
Contributing equally to the editing of the review and initial framework: DeGrado TR, Jensen T
Contributing to the final review, additional statistical analysis in the tables, and editing of all materials and figures: Jensen T

Availability of data and materials

Not applicable.

Financial support and sponsorship
None.

Conflicts of interest
All authors declared that there are no conflicts of interests

Ethical approval and consent to participate
Not applicable.

Consent for publication
Not applicable.

REFERENCES

1. Rinella ME, Lazarus JV, Ratziu V, et al; NAFLD Nomenclature consensus group. A multisociety Delphi consensus statement on new fatty liver disease nomenclature. *Hepatology* 2023;78:1966-86. DOI PubMed PMC
2. Younossi ZM, Golabi P, Paik JM, Henry A, Van Dongen C, Henry L. The global epidemiology of nonalcoholic fatty liver disease (NAFLD) and nonalcoholic steatohepatitis (NASH): a systematic review. *Hepatology* 2023;77:1335-47. DOI PubMed PMC
3. Charlton MR, Burns JM, Pedersen RA, Watt KD, Heimbach JK, Dierkhising RA. Frequency and outcomes of liver transplantation for nonalcoholic steatohepatitis in the United States. *Gastroenterology* 2011;141:1249-53. DOI PubMed
4. Sumida Y, Yoneda M. Current and future pharmacological therapies for NAFLD/NASH. *J Gastroenterol* 2018;53:362-76. DOI PubMed PMC
5. Byrne CD, Targher G. NAFLD: a multisystem disease. *J Hepatol* 2015;62:S47-64. DOI PubMed
6. Shao T, Josephson L, Liang SH. PET/SPECT molecular probes for the diagnosis and staging of nonalcoholic fatty liver disease. *Mol Imaging* 2019;18:1536012119871455. DOI PubMed PMC
7. Wegrzyniak O, Rosestedt M, Eriksson O. Recent progress in the molecular imaging of nonalcoholic fatty liver disease. *Int J Mol Sci* 2021;22:7348. DOI PubMed PMC
8. Trujillo MJ, Chen J, Rubin JM, Gao J. Non-invasive imaging biomarkers to assess nonalcoholic fatty liver disease: a review. *Clin Imaging* 2021;78:22-34. DOI PubMed
9. Pierantonelli I, Svegliati-Baroni G. Nonalcoholic fatty liver disease: basic pathogenetic mechanisms in the progression from NAFLD to NASH. *Transplantation* 2019;103:e1-13. DOI PubMed
10. Younossi ZM, Marchesini G, Pinto-Cortez H, Petta S. Epidemiology of nonalcoholic fatty liver disease and nonalcoholic steatohepatitis: implications for liver transplantation. *Transplantation* 2019;103:22-7. DOI PubMed
11. Ipsen DH, Lykkesfeldt J, Tveden-Nyborg P. Molecular mechanisms of hepatic lipid accumulation in non-alcoholic fatty liver disease. *Cell Mol Life Sci* 2018;75:3313-27. DOI PubMed PMC
12. Milić S, Lulić D, Štimac D. Non-alcoholic fatty liver disease and obesity: biochemical, metabolic and clinical presentations. *World J Gastroenterol* 2014;20:9330-7. DOI PubMed PMC
13. Ekstedt M, Franzén LE, Mathiesen UL, et al. Long-term follow-up of patients with NAFLD and elevated liver enzymes. *Hepatology* 2006;44:865-73. DOI PubMed
14. Singh S, Allen AM, Wang Z, Prokop LJ, Murad MH, Loomba R. Fibrosis progression in nonalcoholic fatty liver vs nonalcoholic steatohepatitis: a systematic review and meta-analysis of paired-biopsy studies. *Clin Gastroenterol Hepatol* 2015;13:643-54. DOI PubMed PMC
15. Ekstedt M, Hagström H, Nasr P, et al. Fibrosis stage is the strongest predictor for disease-specific mortality in NAFLD after up to 33 years of follow-up. *Hepatology* 2015;61:1547-54. DOI PubMed
16. Yatsuji S, Hashimoto E, Tobari M, Taniai M, Tokushige K, Shiratori K. Clinical features and outcomes of cirrhosis due to non-alcoholic steatohepatitis compared with cirrhosis caused by chronic hepatitis C. *J Gastroenterol Hepatol* 2009;24:248-54. DOI PubMed
17. Iqbal U, Perumpail BJ, Akhtar D, Kim D, Ahmed A. The epidemiology, risk profiling and diagnostic challenges of nonalcoholic fatty liver disease. *Medicines* 2019;6:41. DOI PubMed PMC
18. Verma S, Jensen D, Hart J, Mohanty SR. Predictive value of ALT levels for non-alcoholic steatohepatitis (NASH) and advanced fibrosis in non-alcoholic fatty liver disease (NAFLD). *Liver Int* 2013;33:1398-405. DOI PubMed
19. Cusi K, Chang Z, Harrison S, et al. Limited value of plasma cytokeratin-18 as a biomarker for NASH and fibrosis in patients with non-alcoholic fatty liver disease. *J Hepatol* 2014;60:167-74. DOI PubMed
20. Feldstein AE, Wieckowska A, Lopez AR, Liu YC, Zein NN, McCullough AJ. Cytokeratin-18 fragment levels as noninvasive

biomarkers for nonalcoholic steatohepatitis: a multicenter validation study. *Hepatology* 2009;50:1072-8. DOI PubMed PMC
21. Kazankov K, Barrera F, Møller HJ, et al. The macrophage activation marker sCD163 is associated with morphological disease stages in patients with non-alcoholic fatty liver disease. *Liver Int* 2016;36:1549-57. DOI PubMed
22. Nielsen MJ, Nedergaard AF, Sun S, et al. The neo-epitope specific PRO-C3 ELISA measures true formation of type III collagen associated with liver and muscle parameters. *Am J Transl Res* 2013;5:303-15. PubMed PMC
23. Tanwar S, Trembling PM, Guha IN, et al. Validation of terminal peptide of procollagen III for the detection and assessment of nonalcoholic steatohepatitis in patients with nonalcoholic fatty liver disease. *Hepatology* 2013;57:103-11. DOI PubMed
24. Piazzolla VA, Mangia A. Noninvasive diagnosis of NAFLD and NASH. *Cells* 2020;9:1005. DOI PubMed PMC
25. Lin ZH, Xin YN, Dong QJ, et al. Performance of the aspartate aminotransferase-to-platelet ratio index for the staging of hepatitis C-related fibrosis: an updated meta-analysis. *Hepatology* 2011;53:726-36. DOI PubMed
26. Rinella ME, Loomba R, Caldwell SH, et al. Controversies in the diagnosis and management of NAFLD and NASH. *Gastroenterol Hepatol* 2014;10:219-27. PubMed PMC
27. Shah AG, Lydecker A, Murray K, Tetri BN, Contos MJ, Sanyal AJ; Nash Clinical Research Network. Comparison of noninvasive markers of fibrosis in patients with nonalcoholic fatty liver disease. *Clin Gastroenterol Hepatol* 2009;7:1104-12. DOI PubMed PMC
28. Contreras D, González-Rocha A, Clark P, Barquera S, Denova-Gutiérrez E. Diagnostic accuracy of blood biomarkers and non-invasive scores for the diagnosis of NAFLD and NASH: systematic review and meta-analysis. *Ann Hepatol* 2023;28:100873. DOI PubMed
29. López IC, Aroca FG, Bernal MDF, et al. Utility of the ELF test for detecting steatohepatitis in morbid obese patients with suspicion of nonalcoholic fatty liver disease. *Obes Surg* 2017;27:2347-53. DOI PubMed
30. Ratziu V, Massard J, Charlotte F, et al; LIDO Study Group; CYTOL study group. Diagnostic value of biochemical markers (FibroTest-FibroSURE) for the prediction of liver fibrosis in patients with non-alcoholic fatty liver disease. *BMC Gastroenterol* 2006;6:6. DOI PubMed PMC
31. Poynard T, Munteanu M, Charlotte F, et al; FLIP Consortium; the FibroFrance-CPAM Group; the FibroFrance-Obese Group. Diagnostic performance of a new noninvasive test for nonalcoholic steatohepatitis using a simplified histological reference. *Eur J Gastroenterol Hepatol* 2018;30:569-77. DOI PubMed
32. Guajardo-Salinas GE, Hilmy A. Prevalence of nonalcoholic fatty liver disease (NAFLD) and utility of FIBROspect II to detect liver fibrosis in morbidly obese Hispano-American patients undergoing gastric bypass. *Obes Surg* 2010;20:1647-53. DOI PubMed
33. Iruarrizaga-Lejarreta M, Martínez-Arranz I, Morrison M, et al. Targeting the NAFLD metabolome and the shaping of precision medicine for patients with NASH. *J Hepatol* 2018;68:S362-3. DOI
34. Mayo R, Crespo J, Martínez-Arranz I, et al. Metabolomic-based noninvasive serum test to diagnose nonalcoholic steatohepatitis: results from discovery and validation cohorts. *Hepatol Commun* 2018;2:807-20. DOI PubMed PMC
35. Poynard T, Ratziu V, Charlotte F, et al; LIDO Study Group; CYTOL study group. Diagnostic value of biochemical markers (NashTest) for the prediction of non alcoholo steato hepatitis in patients with non-alcoholic fatty liver disease. *BMC Gastroenterol* 2006;6:34. DOI PubMed PMC
36. Dowman JK, Tomlinson JW, Newsome PN. Systematic review: the diagnosis and staging of non-alcoholic fatty liver disease and non-alcoholic steatohepatitis. *Aliment Pharmacol Ther* 2011;33:525-40. DOI PubMed PMC
37. Adams LA, Feldstein AE. Non-invasive diagnosis of nonalcoholic fatty liver and nonalcoholic steatohepatitis. *J Dig Dis* 2011;12:10-6. DOI PubMed
38. Marañón P, Fernández-García CE, Isaza SC, et al. Bone morphogenetic protein 2 is a new molecular target linked to non-alcoholic fatty liver disease with potential value as non-invasive screening tool. *Biomark Res* 2022;10:35. DOI PubMed PMC
39. Neuschwander-Tetri BA, Caldwell SH. Nonalcoholic steatohepatitis: summary of an AASLD Single Topic Conference. *Hepatology* 2003;37:1202-19. DOI PubMed
40. Sorrentino P, Tarantino G, Conca P, et al. Silent non-alcoholic fatty liver disease-a clinical-histological study. *J Hepatol* 2004;41:751-7. DOI PubMed
41. Fracanzani AL, Valenti L, Bugianesi E, et al. Risk of severe liver disease in nonalcoholic fatty liver disease with normal aminotransferase levels: a role for insulin resistance and diabetes. *Hepatology* 2008;48:792-8. DOI PubMed
42. Xia MF, Yki-Järvinen H, Bian H, et al. Influence of ethnicity on the accuracy of non-invasive scores predicting non-alcoholic fatty liver disease. *PLoS One* 2016;11:e0160526. DOI PubMed PMC
43. Eddowes PJ, Sasso M, Allison M, et al. Accuracy of fibroscan controlled attenuation parameter and liver stiffness measurement in assessing steatosis and fibrosis in patients with nonalcoholic fatty liver disease. *Gastroenterology* 2019;156:1717-30. DOI PubMed
44. Jang JK, Lee ES, Seo JW, et al. Two-dimensional shear-wave elastography and us attenuation imaging for nonalcoholic steatohepatitis diagnosis: a cross-sectional, multicenter study. *Radiology* 2022;305:118-26. DOI PubMed
45. Thiagarajan P, Bawden SJ, Aithal GP. Metabolic imaging in non-alcoholic fatty liver disease: applications of magnetic resonance spectroscopy. *J Clin Med* 2021;10:632. DOI PubMed PMC
46. Abrigo JM, Shen J, Wong VWS, et al. Non-alcoholic fatty liver disease: spectral patterns observed from an in vivo phosphorus magnetic resonance spectroscopy study. *J Hepatol* 2014;60:809-15. DOI PubMed
47. Abdelqader A, Goud A, Fleisher AS. Extreme esophageal hyperkeratosis presenting as an arachnoid mass. *Am J Gastroenterol* 2016;111:599. DOI PubMed
48. Allen AM, Shah VH, Therneau TM, et al. Multiparametric magnetic resonance elastography improves the detection of NASH regression following bariatric surgery. *Hepatol Commun* 2020;4:185-92. DOI PubMed PMC

49. Gallego-Durán R, Cerro-Salido P, Gomez-Gonzalez E, et al. Imaging biomarkers for steatohepatitis and fibrosis detection in non-alcoholic fatty liver disease. *Sci Rep* 2016;6:31421. DOI PubMed PMC
50. Andersson A, Kelly M, Imajo K, et al. Clinical utility of magnetic resonance imaging biomarkers for identifying nonalcoholic steatohepatitis patients at high risk of progression: a multicenter pooled data and meta-analysis. *Clin Gastroenterol Hepatol* 2022;20:2451-61.e3. DOI PubMed
51. Papadopoulos V, Baraldi M, Guilarte TR, et al. Translocator protein (18kDa): new nomenclature for the peripheral-type benzodiazepine receptor based on its structure and molecular function. *Trends Pharmacol Sci* 2006;27:402-9. DOI PubMed
52. Masdeu JC, Pascual B, Fujita M. Imaging neuroinflammation in neurodegenerative disorders. *J Nucl Med* 2022;63:45S-52S. DOI PubMed
53. Xie L, Yui J, Hatori A, et al. Translocator protein (18 kDa), a potential molecular imaging biomarker for non-invasively distinguishing non-alcoholic fatty liver disease. *J Hepatol* 2012;57:1076-82. DOI PubMed
54. Li Y, Chen L, Li L, et al. Cholesterol-binding translocator protein TSPO regulates steatosis and bile acid synthesis in nonalcoholic fatty liver disease. *iScience* 2021;24:102457. DOI PubMed PMC
55. Masarone M, Rosato V, Dallio M, et al. Role of oxidative stress in pathophysiology of nonalcoholic fatty liver disease. *Oxid Med Cell Longev* 2018;2018:9547613. DOI PubMed PMC
56. Rokugawa T, Uehara T, Higaki Y, et al. Potential of ^{99m}Tc-MIBI SPECT imaging for evaluating non-alcoholic steatohepatitis induced by methionine-choline-deficient diet in mice. *EJNMMI Res* 2014;4:57. DOI PubMed PMC
57. Mather KJ, DeGrado TR. Imaging of myocardial fatty acid oxidation. *Biochim Biophys Acta* 2016;1861:1535-43. DOI PubMed PMC
58. Giedd KN, Bergmann SR. Fatty acid imaging of the heart. *Curr Cardiol Rep* 2011;13:121-31. DOI PubMed
59. Fukumoto M, Masuda K, Ogawa Y, et al. In vivo imaging of hepatic fatty acid metabolism in patients with nonalcoholic steatohepatitis using semiquantative ^{123}I-BMIPP liver scan. *Hepatol Res* 2005;33:105-9. DOI PubMed
60. Onishi S, Saibara T. In vivo imaging of hepatic fatty acid metabolism in patients with non-alcoholic steatohepatitis using semiquantitative 123I-labeled branched-chain fatty acid analog. *J Gastroenterol Hepatol* 2006;21:S76-8. DOI PubMed
61. Iozzo P, Turpeinen AK, Takala T, et al. Defective liver disposal of free fatty acids in patients with impaired glucose tolerance. *J Clin Endocrinol Metab* 2004;89:3496-502. DOI PubMed
62. Iozzo P, Bucci M, Roivainen A, et al. Fatty acid metabolism in the liver, measured by positron emission tomography, is increased in obese individuals. *Gastroenterology* 2010;139:846-56.e6. DOI PubMed
63. Abele JT, Fung CI. Effect of hepatic steatosis on liver FDG uptake measured in mean standard uptake values. *Radiology* 2010;254:917-24. DOI PubMed
64. Lin CY, Lin WY, Lin CC, Shih CM, Jeng LB, Kao CH. The negative impact of fatty liver on maximum standard uptake value of liver on FDG PET. *Clin Imaging* 2011;35:437-41. DOI PubMed
65. Abikhzer G, Alabed YZ, Azoulay L, Assayag J, Rush C. Altered hepatic metabolic activity in patients with hepatic steatosis on FDG PET/CT. *AJR Am J Roentgenol* 2011;196:176-80. DOI PubMed
66. Bural GG, Torigian DA, Burke A, et al. Quantitative assessment of the hepatic metabolic volume product in patients with diffuse hepatic steatosis and normal controls through use of FDG-PET and MR imaging: a novel concept. *Mol Imaging Biol* 2010;12:233-9. DOI PubMed
67. Keramida G, Potts J, Bush J, Verma S, Dizdarevic S, Peters AM. Accumulation of ^{18}F-FDG in the liver in hepatic steatosis. *AJR Am J Roentgenol* 2014;203:643-8. DOI PubMed
68. Wang G, Corwin MT, Olson KA, Badawi RD, Sarkar S. Dynamic PET of human liver inflammation: impact of kinetic modeling with optimization-derived dual-blood input function. *Phys Med Biol* 2018;63:155004. DOI PubMed PMC
69. Sarkar S, Matsukuma KE, Spencer B, et al. Dynamic positron emission tomography/computed tomography imaging correlate of nonalcoholic steatohepatitis. *Clin Gastroenterol Hepatol* 2021;19:2441-3. DOI PubMed PMC
70. Diehl AM. Nonalcoholic steatosis and steatohepatitis IV. Nonalcoholic fatty liver disease abnormalities in macrophage function and cytokines. *Am J Physiol Gastrointest Liver Physiol* 2002;282:G1-5. DOI PubMed
71. Duman DG, Dede F, Akin H, et al. Colloid scintigraphy in non-alcoholic steatohepatitis: a conventional diagnostic method for an emerging disease. *Nucl Med Commun* 2006;27:387-93. DOI PubMed
72. Sodee DB, Velchic MG, Noto RB, Reilley J, Alavi A. Gastrointestinal system. In: Early PJ, Sodee DB, editors. Principles and practice of nuclear medicine. 2nd ed. St Louis, MO, USA: Mosby; 1995. DOI
73. Subramanian G, McAfee JG, Mehter A, et al. ˆ<99m>Tc-stannous phytate: a new in vivo colloid for imaging the reticuloendothelial system. *J Nucl Med* 1973;14:459. (in Japanese). Available from: https://cir.nii.ac.jp/crid/1570854175563339136. [Last accessed on 10 Aug 2024]
74. Kikuchi M, Tomita K, Nakahara T, et al. Utility of quantitative ^{99m}Tc-phytate scintigraphy to diagnose early-stage non-alcoholic steatohepatitis. *Scand J Gastroenterol* 2009;44:229-36. DOI PubMed
75. Arzoumanian A, Rosenthall L, Seto H. Clinical comparison of 99mTc-labeled preformed phytate colloid and sulfur colloid: concise communication. *J Nucl Med* 1977;18:118-120. PubMed
76. Doughton JA, Hofman MS, Eu P, Hicks RJ, Williams S. A first-in-human study of ^{68}Ga-nanocolloid PET/CT sentinel lymph node imaging in prostate cancer demonstrates aberrant lymphatic drainage pathways. *J Nucl Med* 2018;59:1837-42. DOI PubMed
77. Toi M, Atiqur Rahman M, Bando H, Chow LW. Thymidine phosphorylase (platelet-derived endothelial-cell growth factor) in cancer biology and treatment. *Lancet Oncol* 2005;6:158-66. DOI PubMed

78. Yue H, Belcher AM, Bicak A, Li W. 1211-P: the mechanistic role of thymidine phosphorylase in the development of obesity. *Diabetes* 2021;70:1211-P. DOI
79. Higashikawa K, Horiguchi S, Tarisawa M, et al. Preclinical investigation of potential use of thymidine phosphorylase-targeting tracer for diagnosis of nonalcoholic steatohepatitis. *Nucl Med Biol* 2020;82-3:25-32. DOI PubMed
80. Harrison SA, Bedossa P, Guy CD, et al; MAESTRO-NASH Investigators. A phase 3, randomized, controlled trial of resmetirom in NASH with liver fibrosis. *N Engl J Med* 2024;390:497-509. DOI PubMed
81. Harrison SA, Allen AM, Dubourg J, Noureddin M, Alkhouri N. Challenges and opportunities in NASH drug development. *Nat Med* 2023;29:562-73. DOI PubMed
82. Bravo AA, Sheth SG, Chopra S. Liver biopsy. *N Engl J Med* 2001;344:495-500. DOI PubMed
83. Newsome PN, Sasso M, Deeks JJ, et al. FibroScan-AST (FAST) score for the non-invasive identification of patients with non-alcoholic steatohepatitis with significant activity and fibrosis: a prospective derivation and global validation study. *Lancet Gastroenterol Hepatol* 2020;5:362-73. DOI PubMed PMC
84. Noureddin M, Truong E, Gornbein JA, et al. MRI-based (MAST) score accurately identifies patients with NASH and significant fibrosis. *J Hepatol* 2022;76:781-7. DOI PubMed
85. Jung J, Loomba RR, Imajo K, et al. MRE combined with FIB-4 (MEFIB) index in detection of candidates for pharmacological treatment of NASH-related fibrosis. *Gut* 2021;70:1946-53. DOI PubMed PMC
86. Tavaglione F, Jamialahmadi O, De Vincentis A, et al. Development and validation of a score for fibrotic nonalcoholic steatohepatitis. *Clin Gastroenterol Hepatol* 2023;21:1523-32.e1. DOI PubMed
87. Harrison SA, Ratziu V, Magnanensi J, et al. NIS2+™, an optimisation of the blood-based biomarker NIS4® technology for the detection of at-risk NASH: a prospective derivation and validation study. *J Hepatol* 2023;79:758-67. DOI PubMed
88. Canivet CM, Zheng MH, Qadri S, et al. Validation of the blood test MACK-3 for the noninvasive diagnosis of fibrotic nonalcoholic steatohepatitis: an international study with 1924 patients. *Clin Gastroenterol Hepatol* 2023;21:3097-106.e10. DOI PubMed